Universal features of hydrogen absorption in amorphous transition-metal alloys

J. H. Harris, W. A. Curtin, and M. A. Tenhover
B. P. America,, Corporate Research and Development, 4440 Warrensville Center Road, Cleveland, Ohio 44128
(Received 29 January 1987; revised manuscript received 22 May 1987)

We propose that all $A_{1-x}B_x$ glasses [where A (B) is a late (early) transition metal] are structurally isomorphic, chemically random alloys which store hydrogen in tetrahedral interstitial sites $A_{4-n}B_n$ (in decreasing order $n=4,3,2,\ldots$). The maximum absorbed hydrogen-to-metal atomic ratio *within each type of interstitial site* is $1.9\binom{4}{n}x^n(1-x)^{4-n}$ [$\binom{4}{n}=4!/n!(4-n)!$] independent of alloy and temperature. The chemical potential as a function of hydrogen concentration within a single site type n is also independent of composition and temperature. The only *nonuniversal* feature is the dependence of the typical site energies E_n of the type-n sites on the A and B atoms, which may, however, be estimated from crystalline hydride properties. This model agrees with our electrochemical measurements of hydrogen in Ni-Zr, Pd-Ti, and Ni-Ti, predicts total H/M ratios for Ni-Zr and Cu-Ti alloys in excellent agreement with literature gas-phase data over a wide range of compositions and thermodynamic conditions, and is consistent with literature H/M data on other alloys at isolated compositions. We show theoretically that infinite near-neighbor hydrogen-hydrogen interactions (blocking) in a glass dominated by fivefold rings of tetrahedral units predicts the observed x dependence of H/M with a prefactor of 1.9–2.1, in excellent agreement with the observed factor of 1.9. This result supports theoretical models of icosahedral ordering in glasses.

I. INTRODUCTION

In the past ten years, a large number of papers have been published investigating the hydrogen-storage properties of early-transition-metal–late-transition-metal (ETM-LTM) amorphous alloys. A wide range of gas-phase measurements have been performed which monitor hydrogen-storage capacities as a function of hydrogen-gas pressure. Materials probed in these studies include the alloys Ni-Zr,[1,2] Cu-Ti,[3,4] Pd-Zr,[5] Rh-Zr,[5] Cu-Zr,[6] and Fe-Ti.[7] By combining gas-phase charging with a careful x-ray diffraction study, Samwer and Johnson[5] were able to identify two distinct tetrahedral sites as the most likely candidates to store hydrogen in Pd-Zr and Rh-Zr glasses. By monitoring Zr-Zr distances as a function of hydrogen loading, these workers concluded that hydrogen is likely to reside in interstitial tetrahedral sites consisting of four Zr atoms (Zr_4) and possibly in sites with three Zr atoms and one Pd or Rh atom ($PdZr_3$) under the conditions of their experiment. Rush *et al.*[8] had similar conclusions concerning Cu-Ti glasses which they investigated with neutron scattering. Their results indicate that the hydrogen site consists of a tetrahedral interstitial with four Ti nearest neighbors. In addition, the width of their scattering peak indicates that significant variation in the hydrogen local environment exists. Similar conclusions obtained from neutron and x-ray studies are found in Refs. 9 and 10. Evidence for this site-to-site variation has been found in internal-friction measurements[11] and chemical-potential measurements[12] as well. In addition to these static measurements, a large body of literature addressing the dynamics of hydrogen in amorphous alloys exists.[13] For ETM-LTM glasses, these studies indicate a widely varying diffusion coefficient with hydrogen content. Again, this is interpreted as further evidence for a wide variation in hydrogen-site energies.

Interactions between hydrogen atoms in amorphous materials have been proposed as a means to limit the number of occupiable sites in the glass. In crystalline hydrogen-storage materials a variety of hydrogen-hydrogen interactions have been postulated. At short distances (<2.1 Å), a strong repulsive interaction drastically limits the total site occupation, the so-called Switendick criterion.[14] Sawmer and Johnson[5] applied this concept to near-neighbor hydrogen sites in their study of amorphous Pd-Zr and Rh-Zr alloys in an attempt to explain why all possible tetrahedral sites of a particular identity (e.g., Zr_4) are not accessible to hydrogen. Batalla *et al.*[2] assumed the same general interaction but with variable range to best fit their experimental data on Ni-Zr. Although the inclusion of infinite interactions did limit the total hydrogen content, detailed agreement with experiment in both cases was only fair.

As is indicated by this Introduction, a good deal of experimental effort has been devoted toward understanding the nature of hydrogen in amorphous metal alloys. The general features which emerge from the literature show that hydrogen is stored in sites with tetrahedral symmetry and varying chemical identity (e.g., Zr_4, Zr_3Pd), that the energies of these sites are broadened due to disorder, and that some type of short-range blocking mechanism may limit the number of occupiable tetrahedra. Other than these trends, no consistent and general model has been proposed which explains the details of hydrogen storage in this class of materials. A successful model for hydrogen storage in these glasses must address a number of key issues: (i) the identity of hydrogen interstitial

sites, (ii) the factors influencing the occupation of these sites with changing hydrogen content and alloy composition, (iii) the dependence of hydrogen concentration on alloy composition and thermodynamic conditions (such as external H_2-gas pressure), (iv) the interactions between interstitial hydrogens atoms, and (v) all of the above as a function of the ETM and LTM constituents.

Motivated by our electrochemical measurements of the hydrogen chemical potential in amorphous Ni-Zr and Pd-Ti alloys, we present a universal picture of hydrogen storage in ETM-LTM glassy alloys which answers all of the above questions. In an $A_{1-x}B_x$ glassy alloy (A = Ni, Pd, Cu; B = Ti, Zr), we find that hydrogen is absorbed into distinct tetrahedral interstitial sites which consists of four B atoms (B_4), three B atoms and one A atom (AB_3) and, *in many glasses at STP*, two B atoms and two A atoms (A_2B_2). The amount of hydrogen per metal atom which can be stored in each type of tetrahedral site is proportional to the number of those tetrahedral sites in a chemically random glass [i.e., proportional to x^4 for B_4, $4x^3(1-x)$ for AB_3, and $6x^2(1-x)^2$ for A_2B_2] with a *universal* (composition, site-type, and alloy-type independent) proportionality factor of 1.9. The energetics of hydrogen in a given $A_{1-x}B_x$ glass, which determines what types of sites may be occupied by hydrogen at given thermodynamic conditions, is independent of composition and may be estimated from the hydriding energies of the constituent crystalline metal elements. Our general picture is consistent with a wide range of available literature data on the hydrogen capacities of ETM-LTM glasses as a function of composition, pressure, and temperature. Furthermore, the universal proportionality factor of 1.9–2.1 is obtained theoretically with the introduction of infinite near-neighbor hydrogen-hydrogen interactions in a chemically random $A_{1-x}B_x$ alloy in which fivefold rings of tetrahedra are the main structural feature.

The details of our electrochemical experiment and a presentation of the key results of our chemical-potential measurements are contained in Sec. II. Section III comprises a detailed description of our model and the application of this model to explain a wide range of literature data. In Sec. IV we show that infinite nearest-neighbor hydrogen-hydrogen interactions limit hydrogen storage in each type of site to a composition-independent fraction of the number of interstitial sites available. In Sec. V we discuss a number of important implications that our picture of hydrogen storage has on glassy hydrides and on the nature of the amorphous state itself.

II. EXPERIMENT

A metallic alloy can be charged or discharged with atomic hydrogen introduced from either a gas phase or an electrochemical (aqueous) environment. In the gas phase, the surface of the metal is exposed to a pressure of hydrogen gas. H_2 molecules dissociate on the alloy surface, and atomic hydrogen subsequently diffuses into the metallic lattice. In an electrochemical experiment, the alloy is cathodically biased in an aqueous electrolyte. For alkaline electrolytes, the applied bias electrolyzes water into a hydrogen atom adsorbed on the electrode surface and a hydroxyl ion in solution. The adsorbed hydrogen atom then diffuses into the bulk of the alloy. In the gas-phase experiment, equilibrium is established between hydrogen dissolved in the metal and hydrogen gas, allowing the hydrogen chemical potential relative to a reference state (usually H_2 at $T=25\,^{\circ}\mathrm{C}$ and $P=1$ atm) to be obtained simply from the measured gas pressure. In the electrochemical experiment, the open-circuit electrode potential relative to a reference state plays a role similar to the logarithm of the gas pressure and allows for a determination of the hydrogen chemical potential relative to a reference reaction. One advantage of the electrochemical approach is that a range of hydrogen chemical potential can be accessed corresponding to extremely low H_2 pressures in a gas-phase measurement, and with high accuracy (typical chemical-potential changes of less than 1 kJ/mol H_2 can easily be measured). We have chosen the electrochemical method for studying hydrogen in amorphous metal alloys because accurate determinations of chemical potential in this "low-pressure" regime are important. A disadvantage of the electrochemical method is that in certain ranges of electrochemical potential other competing electrochemical reactions occur, such as electrode oxidation or hydrogen-gas evolution. These competing reactions impose limits on the range of chemical potential we can interrogate electrochemically.

In this series of experiments, we have used the electrochemical technique to determine hydrogen content in a series of amorphous metal alloys as a function of alloy composition and hydrogen chemical potential (μ) at room temperature. In an electrochemical cell, relative chemical potentials can be directly measured by monitoring the cell voltage. The Gibbs-free-energy difference between two half-cell reactions is given by

$$G=-nFE\ , \tag{2.1}$$

where E is the potential difference between the two reactions, n is the number of moles which react, and F is Faraday's constant.[15] In this experiment, we wish to measure the chemical potential of hydrogen dissolved in the alloy relative to a standard state of one atmosphere hydrogen gas. The appropriate overall reaction, which facilitates direct comparison between electrochemical and gas-phase data, is

$$2\mathrm{M}+\mathrm{H_2}\leftrightarrow 2\mathrm{MH}\ , \tag{2.2}$$

where M is a metal atom. In an alkaline electrolyte, the charge or discharge of the metallic alloy with hydrogen is described by the electrochemical reaction

$$\mathrm{H_2O}+\mathrm{M}+e^-\leftrightarrow \mathrm{MH}+\mathrm{OH}^-\ . \tag{2.3}$$

By choosing the reversible hydrogen electrode (RHE) as our electrochemical reference, the change in Gibbs free energy obtained from the measured cell voltage via Eq. (2.1) yields the free-energy change between the two sides of reaction (2.2). Thus experimentally we measure the potential difference under open-circuit conditions between the amorphous metal alloy with various concen-

trations of hydrogen, and a hydrogen-evolving electrode under the same conditions of temperature, pressure, and *p*H (the RHE reference).

Our amorphous metal electrodes were fabricated either from sputtered films on nickel substrates (Pd-Ti, Ni-Ti samples) or from rapidly quenched ribbons (Ni-Zr). In the case of rapidly quenched samples, the ribbons were first etched to remove any surface oxide and then ground into coarse powders. These powders were pressed with Ni metal as a binder into flat pellets. Ni is chosen as a binding material because it is stable in the alkaline electrolyte and does not absorb hydrogen under the conditions of this experiment. The flat pellets were formed into electrodes using nickel foil and fine nickel screen for electrical contact. All samples tested were verified to be completely amorphous using x-ray diffraction. Compositions were checked with photoelectron spectroscopy and Rutherford backscattering spectroscopy.

Our experimental setup consists of an electrochemical cell with a nickel hydroxide counterelectrode, a RHE reference, and an electrolyte of 4*N* KOH. The amorphous-metal-alloy sample serves as the working electrode. All charging and discharging functions are performed using a Keithley programmable current source controlled by an IBM personal computer. Initially the amorphous metal is charged until hydrogen gas evolves off the electrode surface. This hydrogen-evolution reaction (at a pressure of 1 atm) provides an upper limit $\mu_{\max}=-38.5$ kJ/mol H_2 (relative to the H_2 binding energy) on the attainable hydrogen chemical potential. At this point the current is terminated and an open-circuit voltage relative to the RHE reference electrode is measured. A current pulse is then applied to the amorphous alloy to *extract* a known amount of hydrogen. The number of hydrogen atoms desorbed from the metal is easily counted since each electron passing through the electrode corresponds to one hydrogen atom [see Eq. (2.3)]. After inducing this change in hydrogen concentration in the alloy, a rest potential measurement is made to obtain the chemical potential at the new hydrogen concentration. Care must be taken to insure that the hydrogen is equilibrated within the alloy before this measurement is taken. Since the equilibration time increases (diffusion coefficient decreases) very rapidly with decreasing hydrogen content, the discharge current (or rate at which hydrogen is extracted) is also decreased at lower hydrogen concentrations, with a total change of about a factor of 20. The measurement is terminated when the equilibrium time is on the order of 5 h, where the integrated leakage current (due to dissolved oxygen recombining with hydrogen on the alloy surface) becomes a source of error. While the upper chemical-potential limit $\mu_{\max}=-38.5$ kJ/mol H_2 is set by H_2 evolution, these kinetic effects limit the minimum obtainable chemical potential to $\mu_{\min}=-100$ kJ/mol H_2. Sites with $\mu<\mu_{\min}$ are filled during the initial charge and remain filled during the experiment. Thus, at an arbitrary chemical potential $\mu>\mu_{\min}$ the amount of hydrogen absorbed or desorbed in our electrochemical experiment is given by

$$\Delta H/M(\mu)=H/M(\mu)-H/M(\mu_{\min}) ,$$

where $H/M(\mu)$ is the *total* number of hydrogen atoms divided by the number of metal atoms, absorbed at chemical potential μ. Over the entire experimentally accessible range of μ, we measure a total *change* in hydrogen content

$$\Delta H/M\mid_{\text{expt}}=H/M(\mu_{\max})-H/M(\mu_{\min}) . \tag{2.4}$$

In Fig. 1, we show a plot of chemical potential μ versus $[\Delta H/M(\mu)]/[\Delta H/M\mid_{\max}]$ ($\Delta H/M\mid_{\max}$ is a quantity that is proportional to $\Delta H/M\mid_{\text{expt}}$) for various rapid quenched $Ni_{1-x}Zr_x$ alloys. The origin of the proportionality between $\Delta H/M\mid_{\text{expt}}$ and $\Delta H/M\mid_{\max}$ is discussed in the next section. Although the lower limit $\mu_{\min}=-100$ kJ/mol H_2 is due to kinetic limitations, the sharp decrease in μ with decreasing $\Delta H/M$ is indicative of a *depletion* of available hydrogen sites. The hydrogen sites with $\mu>-100$ kJ/mol H_2 are thus physically distinguished from those sites in the range $\mu<-100$ kJ/mol H_2 which are not probed here. Because of this distinguishability, the experimental lower limit $\mu_{\min}$ is *not* a limitation to the study of the distinct group of sites at energies above $\mu_{\min}$. Having normalized by $\Delta H/M\mid_{\max}$ and formed a concentration (to within a scale factor), we observe that μ versus concentration exhibits *universal* (composition-independent) behavior.

The variation with composition x in total hydrogen content $\Delta H/M\mid_{\text{expt}}$ over the experimental range of μ is shown in Fig. 2 for the amorphous-metal-alloy systems Pd-Ti and Ni-Zr. The compositional dependence of the hydrogen capacity in this range of μ allows one to identify the interstitial sites being occupied in each of these alloys as tetrahedral interstitials of *distinct chemical composition*. For example, in the $Ni_{1-x}Zr_x$ system within the range of chemical potential probed (-100 kJ/mol $H_2<\mu<-38.5$ kJ/mol H_2), the total change in

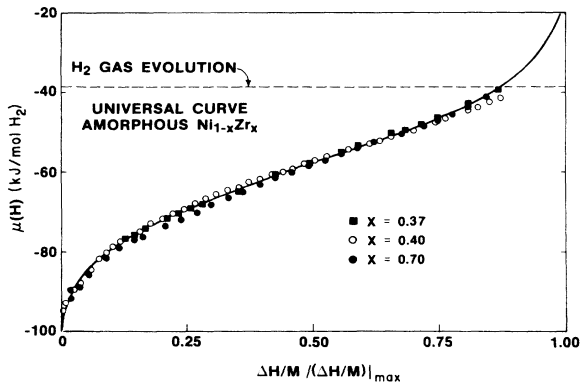

FIG. 1. Chemical potential μ of hydrogen in $Ni_{1-x}Zr_x$ vs total normalized hydrogen-to-metal ratio $(\Delta H/M)/(\Delta H/M\mid)_{\max}$ at compositions $x=0.37$, 0.4, and 0.7. The upper limit $\mu_{\max}=-38.5$ kJ/mol H_2 corresponds to the standard chemical potential of H_2 gas at $T=295$ K, $P=1$ atm. The rapid decrease in μ at low concentration is indicative of a depletion of available hydrogen sites in this range of free energy.

hydrogen storage $\Delta H/M\mid_{\text{expt}}$ is proportional to the function $x^2(1-x)^2$, as indicated by the dashed line in Fig. 2. This dependence over a wide range of x indicates that the site storing hydrogen in this energy range is a *tetrahedral interstitial comprised of 2 Ni and 2 Zr atoms.* Although tetrahedral hydrogen sites have been proposed previously, only Zr_4 and $NiZr_3$ sites have been considered to store hydrogen.[2,5,10] We have the first evidence that Ni_2Zr_2 sites store a nontrivial amount of hydrogen (up to at least $H/M=0.6$) in amorphous Ni-Zr. In general, we observe the hydrogen content $\Delta H/M\mid_{\text{expt}}$ to scale with x in proportion to the number of $A_{4-n}B_n$ tetrahedral structural units which occur in a *chemically random* alloy

$$\Delta H/M\mid_{\text{expt}}=1.7\begin{pmatrix}4\\n\end{pmatrix}x^n(1-x)^{4-n} \tag{2.5}$$

in the $A_{4-n}B_n$ sites, where $\binom{4}{n}=4!/n!(4-n)!$ is the nth coefficient in the expansion of $[x+(1-x)]^4$. It is important to note that the factor of $\simeq 1.7$ is obtained *independent of* n with $n=2$ for Ni-Zr as discussed above, and $n=3$ for Pd-Ti. The validity of this assertion is illustrated in Fig. 2, where Eq. (2.5) is plotted (along with our experimental data) for $n=2$ and $n=3$. The distinguishability of interstitial sites of distinct chemical composition, a universal chemical potential as a function of hydrogen concentration, and the general proportionality factor of 1.7 are important observations which a model for hydrogen storage in these materials must address.

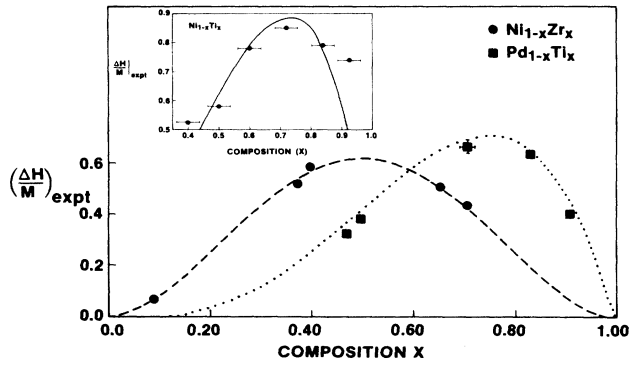

FIG. 2. Total hydrogen content over the range of μ probed, $\Delta H/M\mid_{\text{expt}}$, as a function of ETM composition x for both $Ni_{1-x}Zr_x$ and $Pd_{1-x}Ti_x$. Also shown are the curves $\Delta H/M\mid_{\text{expt}}=10.2x^2(1-x)^2$ and $\Delta H/M\mid_{\text{expt}}=6.8x^3(1-x)$ which are fit to the Ni-Zr and Pd-Ti data, respectively. These proportionalities imply that Ni-Zr stores hydrogen in Ni_2Zr_2 tetrahedral interstitial sites while Pd-Ti stores hydrogen in $PdTi_3$ sites in this range of chemical potential. Inset: $\Delta H/M\mid_{\text{expt}}$ measured electrochemically for $Ni_{1-x}Ti_x$ over the same range of μ as in Fig. 1. Also shown is the predicted hydrogen content consisting of a sum of the full contribution $1.9[4x^3(1-x)]$ from the $NiTi_3$ sites (as in Pd-Ti) and a fractional contribution of $0.2\{1.9[6x^2(1-x)^2]\}$ of the Ni_2Ti_2 sites (as in Ni-Zr).

III. MODEL FOR HYDROGEN STORAGE IN AMORPHOUS ALLOYS

Based on our experimental observations, we propose the following model for hydrogen storage in late and early transition metal alloys $A_{1-x}B_x$. We consider the glass to be a chemically *random alloy* (no chemical short-range order) with a structure composed of packed, distorted tetrahedra. We label each tetrahedron by the types of metal atoms at its vertices (B_4, AB_3, A_2B_2, A_3B, A_4, or, generally, $A_{4-n}B_n$). The number of each type of tetrahedra is thus proportional to the probability of choosing n B and $4-n$ A atoms from a distribution of B and A atoms consistent with the overall alloy composition (having a fraction x of B atoms), i.e., proportional to the nth term in the expansion of $[x+(1-x)]^4$. Hydrogen interstitial sites are located at the "centers" of these tetrahedral units and (i) may thus also be labelled by the identities of the four atoms at the vertices and (ii) occur with the same probabilities as the tetrahedra. Each hydrogen interstitial site is also fourfold coordinated with neighboring interstitial sites. The predominance of tetrahedral interstitials has been verified for the computer-generated relaxed, one-component random close-packed structure.[16] Now, the energetics of a hydrogen atom at a particular site is supposed dominated by the *local* metallic environment (the four neighboring metal atoms). The lowest-energy hydrogen sites are those surrounded by four early-transition-metal atoms, so that $E_4<E_3<E_2<E_1<E_0$ (E_n is the energy corresponding to an hydrogen in an $A_{4-n}B_n$ interstitial site). This ordering of energies is consistent with the large exothermic heats of formation of ETM hydrides relative to those of the LTM hydrides, which suggests a preference for maximizing ETM-hydrogen coordination in the alloy. Both the existence of tetrahedral interstitials and the preference of B-H coordination have been previously substantiated by many neutron and x-ray diffraction studies.[1,2,5,10] Since the hydrogen binding energy is predominantly electronic in origin,[14] we assume the energetics of hydrogen in the metal is independent of temperature. The domination of the local environment also implies that the energies E_n are x independent, with only the numbers of each type of site changing with x.

Due to the range of distortions about ideal tetrahedral structure in the local glass environment, fluctuations in the hydrogen-site energies must exist.[17] This leads to distributions in the site energies about the mean, typical site energies E_n which we characterize by half widths at half maximum σ_n. The ability to experimentally distinguish the occupation of different types of sites (e.g., to see the Ni_2Zr_2 sites as distinct from the $NiZr_3$ sites in Ni-Zr) dictates that the widths be narrower than the *differences* between mean site energies, $\sigma_n+\sigma_{n-1}<|E_n-E_{n-1}|$. Finally, we consider the structural fluctuations which generate the widths to be independent of composition.

Our picture may be summarized by stating that the density of states (DOS) for hydrogen atoms in the glass, $g(E,x,T)$, may be decomposed into a sum of contributions from sites of each type as

$$g(E,x,T)=\sum_n f_n(x)g_n(E) , \tag{3.1}$$

where $f_n(x)$ is *proportional to* $\binom{4}{n}x^n(1-x)^{4-n}$. The function $f_n(x)$, which contains all the x dependence of $g(E,x,T)$, is the nth term in $[x+(1-x)]^4$. The $g_n(E)$ are the DOS for the type-n sites only (characterized by E_n and σ_n) and are normalized to unity, nonoverlapping and independent of both temperature and composition. Also, $g(E,x,T)$ is taken to be independent of T. Using this DOS picture one can understand why only *one* type of site is observed in the electrochemical experiment (e.g., Ni_2Zr_2). Since the measurement is restricted to a window of chemical potential, if the range $\mu_{\min}<\mu<\mu_{\max}$ predominantly overlaps only one peak in the DOS, those sites dominate the electrochemical results. The lower energy sites (e.g., Zr_4, $NiZr_3$) are occupied but not probed in this measurement. Figure 3 shows a schematic of the hydrogen DOS $g(E,x,T)$ as a function of energy for $Ni_{1-x}Zr_x$ at the composition $x=0.6$. The window of chemical potential measured electrochemically is indicated on this figure.

We now consider the variations in hydrogen content and chemical potential with composition which are predicted by this model. At low temperatures [$RT\ll\sigma_n$, entropic effects enter at order $(RT/\sigma_n)^2$], the *total* hydrogen content per metal atom at chemical potential μ is simply

$$H/M(\mu)=N\int_{-\infty}^{\mu} dE\, g(E,x,T) , \tag{3.2}$$

where N is the number of interstitial sites per metal atom. Over a specific range of chemical potential $\mu_{\min}$ to μ, extending only over a single peak $g_n(E)$ as indicated in Fig. 3, the hydrogen content is

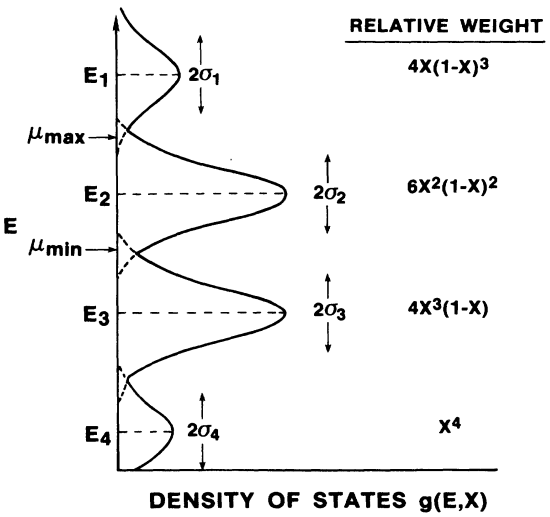

FIG. 3. Schematic of the density of states $g(E,x,T)$ for hydrogen in tetrahedral interstitial sites. $g(E,x,T)$ consists of a sum of contributions $g_n(E)$ from the different types n of tetrahedra, where E_n corresponds to the typical energy of a $A_{4-n}B_n$ interstitial site. The relative weight under each peak is proportional to the probability of occurence of a type-n site in a random alloy.

$$\Delta H/M=Nf_n(x)\int_{\mu_{\min}}^{\mu} dE\, g_n(E) . \tag{3.3}$$

Normalizing by the maximum hydrogen capacity of the type-n sites,

$$\Delta H/M\mid_{\max}=Nf_n(x)\int_{-\infty}^{\infty} dE\, g_n(E)\equiv Nf_n(x) \tag{3.4}$$

we obtain

$$(\Delta H/M)/(\Delta H/M\mid_{\max})=\int_{\mu_{\min}}^{\mu} dE\, g_n(E) . \tag{3.5}$$

The total hydrogen content over the experimental range $\mu_{\min}$ to $\mu_{\max}$ is

$$\begin{aligned}\Delta H/M\mid_{\text{expt}}&=Nf_n(x)\int_{\mu_{\min}}^{\mu_{\max}} dE\, g_n(E)\\&=\Delta H/M\mid_{\max}\int_{\mu_{\min}}^{\mu_{\max}} dE\, g_n(E) .\end{aligned} \tag{3.6}$$

Inverting Eq. (3.5) we find that μ versus $\Delta H/M$ normalized by *either* $\Delta H/M\mid_{\text{expt}}$ or $\Delta H/M\mid_{\max}$ is predicted to be independent of composition x (and also temperature), in agreement with the experimental results of Fig. 1. The aspects of our model which lead to this conclusion are the x independence of E_n and σ_n [and hence $g_n(E)$]. Furthermore, the hydrogen content $\Delta H/M\mid_{\text{expt}}$ given by Eq. (3.6) is *proportional to* $f_n(x)$ and hence to $\binom{4}{n}x^n(1-x)^{4-n}$, also in agreement with our results shown in Fig. 2. This result follows from the assumption of a *chemically random* alloy with tetrahedral sites of each type which are well separated in energy.

The origin of the proportionality factor appearing in Fig. 1 now becomes apparent as the difference between $\Delta H/M\mid_{\text{expt}}$ and $\Delta H/M\mid_{\max}$ in Eq. (3.6) and is equal to the fraction of type-n sites probed experimentally. To obtain an estimate of this fraction, we use a normalized Gaussian centered on E_2 and of e^{-1} width σ_2 to approximate $g_2(E)$ for the Ni-Zr system. We obtain the excellent fit shown as the solid line in Fig. 1 for the parameter values $E_2=-58.5$ kJ/mol and $\sigma_2=25.0$ kJ/mol (N.B. $RT\ll\sigma_n$). We conclude, as evident in Fig. 1, that the experiment does not probe the full range of $g_2(E)$, but rather only about 90% of the sites, so that

$$\int_{\mu_{\min}}^{\mu_{\max}} dE\, g_2(E)\approx 0.9 . \tag{3.7}$$

We find only $\leq 1\%$ of the Ni_2Zr_2 sites lie below $\mu_{\min}$, so the $\mu_{\min}$ limit has little effect on the measured Ni_2Zr_2 occupation. The maximum hydrogen capacity $\Delta H/M\mid_{\max}=Nf_n(x)$ of the Ni_2Zr_2 ($n=2$) sites is thus slightly larger (10%) than we directly measure using the electrochemical technique because of the experimental upper limit of $\mu_{\max}$. Our normalization of $\Delta H/M$ by $\Delta H/M\mid_{\max}=(\Delta H/M\mid_{\text{expt}})/0.9$ in Fig. 1 transforms the measured $\Delta H/M$ into a true *concentration* (fraction of occupied type-n sites) of the Ni_2Zr_2 sites.

Since the window of experimentally accessible chemical potentials is limited to $\mu_{\min}=-100$ kJ/mol and $\mu_{\max}=-38.5$ kJ/mol, the type of site probed electrochemically must have a mean energy E_n falling within that window. For Ni-Zr, we find that it is the Ni_2Zr_2 sites which are probed and we have determined a mean energy for these sites of $E_2=-58.5$ kJ/mol. We are

able to correlate the typical site energies observed with a simple weighted average of the enthalpies of formation $\mathcal{H}_0$ of the pure crystalline hydrides BH_2 and AH,[18]

$$E_n=[n\mathcal{H}_0(BH_2)+(4-n)\mathcal{H}_0(AH)]/4$$

as shown in Table I. Pd has an anomalously low (negative) hydride heat of formation, storing hydrogen in octahedral interstitial sites because of its open structure, so we assume that Pd in a glassy alloy behaves more like Ni than crystalline Pd. The simple average implies that in our experiments the Ni_2Zr_2 sites in Ni-Zr are accessed while the $PdTi_3$ and possibly some Pd_2Ti_2 sites are accessed in Pd-Ti. Our experimentally derived E_2 in Ni-Zr is about 15 kJ/mol positive of the estimate obtained by averaging, which suggests that the Pd_2Ti_2 sites in Pd-Ti are also actually at energies higher than estimated and perhaps outside of the accessible range of energies, consistent with our observations. A consequence of the rough accuracy of the simple average is that we also obtain limits on the widths of the DOS peaks. Since $\Delta H/M\mid_{\text{expt}}$ follows the random statistics $\binom{4}{n}x^n(1-x)^{4-n}$ for a particular n in a given alloy, the peaks must be narrower than the separations between peaks, as remarked earlier and as indicated in Fig. 3. However, the separations between peaks may now be estimated by the simple averaging as

$$E_n-E_{n-1}=[\mathcal{H}_0(BH_2)-\mathcal{H}_0(AH)]/4\ .$$

For Ni-Zr, the widths are thus bounded by approximately $\sigma_n \lesssim 25$ kJ/mol (which is about equal to the measured width obtained above). Similar widths follow for the $PdTi_3$ sites in Pd-Ti and hence we expect about 90% of these sites are accessed in our experiments.

We now address the issue of the maximum hydrogen content within each type of site in these alloys. We make the proportionality of $f_n(x)$ to $\binom{4}{n}x^n(1-x)^{4-n}$ explicit by *defining* $f_n(x)=\alpha\binom{4}{n}x^n(1-x)^{4-n}$, so that

$$\Delta H/M\mid_{\max}=Nf_n(x)=N\alpha\begin{bmatrix}4\\n\end{bmatrix}x^n(1-x)^{4-n}\ . \quad (3.8)$$

Recalling Eq. (2.5)

$$\Delta H/M\mid_{\text{expt}}=1.7\begin{bmatrix}4\\n\end{bmatrix}x^n(1-x)^{4-n} \quad (2.5)$$

and using Eqs. (3.6) and (3.7) (to account for the experimental limitation of approximately 90% filling of the Ni_2Zr_2 and $PdTi_3$ sites discussed above), we find

$$N\alpha\equiv N_{\text{eff}}=1.7/0.9=1.9\ . \quad (3.9)$$

N_{eff} is *independent of composition, type of alloy,* or *type of site probed.* We assert that the factor of 1.9 is the *effective* number of interstitial sites per metal atom available for hydrogen occupation. It is also the appropriate prefactor in Eq. (3.8) for the number of occupiable hydrogen sites per metal atom *for each type of site n* in this class of metallic glasses. With this value of $N\alpha$, we now *predict* that the total H/M at chemical potential μ, composition x, and temperature $RT\ll\sigma_n$ is

TABLE I. Weighted average of hydride formation enthalpies $\mathcal{H}_0$ of the constituent-atom crystalline hydrides BH_2 and AH, $E_n=[n\mathcal{H}_0(BH_2)+(4-n)\mathcal{H}_0(AH)]/4$ as an estimate of hydrogen enthalpy in an $A_{4-n}B_n$ tetrahedral site, for a variety of ETM/LTM alloys.

	Site type			
A-B	B_4	AB_3	A_2B_2	A_3B
Ni-Zr	−162	−117	−73	−28
Pd-Zr	−162	−117	−73	−28
Rh-Zr	−162	−112	−62	−12
Ni-Ti	−124	−89	−50	−18
Pd-Ti	−124	−89	−50	−18
Fe-Ti	−124	−85	−45	−6
Ni-Hf	−133	−96	−58	−21

$$H/M(\mu)=1.9\sum_n\begin{bmatrix}4\\n\end{bmatrix}x^n(1-x)^{4-n}\int_{-\infty}^{\mu}dE\,g_n(E)\ . \quad (3.10)$$

The validity of this prediction for total H/M, which is one of the key results of this paper, is examined in some detail below.

Gas-phase experiments on the Ni-Zr system measure the *total* hydrogen concentration as a function of pressure P and T. At a given P and T, the chemical potential of the metal-hydrogen system (in kJ/mol H_2) is equal to that of the gas,

$$\mu=\mu_{H_2}=-TS(T)+RT\ln(P)\ ,\quad P\text{ in atm}\ , \quad (3.11)$$

where $S(T)$ is the entropy of H_2 gas at temperature T.[18] Over the range of P and T probed in gas-phase experiments, μ is limited to the same range as in our electrochemical measurements, $-100\text{ kJ/mol}\lesssim\mu\lesssim-38.5$ kJ/mol. However, in contrast to our electrochemical experiments, the total $H/M(\mu)$ is measured, which corresponds to having a lower limit of $\mu_{\min}=-\infty$. For Ni-Zr, our model thus predicts, using Eq. (3.10), a *total* hydrogen-to-metal ratio of

$$H/M(\mu)=1.9[x^4+4x^3(1-x)+6x^2(1-x)^2c_2(\mu)]\ ,$$
$$-100\text{ kJ/mol}<\mu<-38.5\text{ kJ/mol}\ , \quad (3.12)$$

where $c_2(\mu)$ is given by the universal curve of Fig. 1, and μ is related to P and T via Eq. (3.10). Thus, *with no free parameters,* we predict total hydrogen content for $Ni_{1-x}Zr_x$ alloys using Eq. (3.12). Our predictions are compared to the gas phase data of Aoki *et al.*[1] in Figs. 4 and 5. In Fig. 4, for example, the data was obtained at $T=523$ K and $P=50$ atm, so that $\mu=-59.6$ kJ/mol and hence, from Fig. 1, $c_2(\mu=-59.6\text{ kJ/mol})=0.48$ independent of composition x. Over a wide variation in temperature (373–573 K), pressure (0.1–50 atm), and composition x ($0.1<x<0.7$), Eq. (3.12) is in *excellent* agreement (0–15 %) with independent experimental results. Therefore $N_{\text{eff}}=1.9$ and the random-alloy statistics are correct for *all* occupied sites (Zr_4, $NiZr_3$, and Ni_2Zr_2) in this system. In addition, the accuracy of our predictions for total H/M over a wide range of tempera-

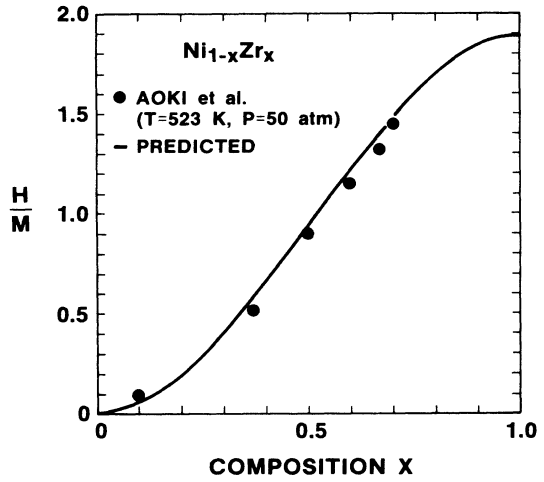

FIG. 4. Total hydrogen-to-metal ratio H/M in $Ni_{1-x}Zr_x$ as predicted (——) and obtained experimentally [●, Ref. 1(a)] at $T=523$ K, $P=1$ atm over a wide range of compositions x. The predicted H/M has no free parameters and is given by $H/M=1.9[x^4+4x^3(1-x)+6x^2(1-x)^2c_2(\mu)]$ with $c_2(\mu=-59.6)$ obtained from the universal curve in Fig. 1.

tures using the universal curve obtained at $T=295$ K is further evidence for the temperature independence of the hydrogen energetics in the metallic alloy.

We have also studied Ni-Ti alloys electrochemically. From simple averaging considerations (see Table I), this glass is expected to store hydrogen in $NiTi_3$ sites and possibly some Ni_2Ti_2 sites within the range of -100 kJ/mol $<\mu<-38.5$ kJ/mol available experimentally. The inset of Fig. 2 shows our measurements of $\Delta H/M\mid_{\text{expt}}$ versus x. A detailed chemical potential versus concentration curve has not been measured and so it is not known whether any $NiTi_3$ sites lie *below* $\mu_{\min}$ (recall only 1% of the Ni_2Zr_2 sites are below $\mu_{\min}$). We assume all the $NiTi_3$ sites lie above $\mu_{\min}$ and below $\mu_{\max}$ and fit our data using

$$\Delta H/M\mid_{\text{expt}}=1.9[4x^3(1-x)+6x^2(1-x)^2c_2(\mu_{\max})] \tag{3.13}$$

with the *single* adjustable parameter $c_2(\mu_{\max})=0.2$ to account for the fractional occupation of the Ni_2Ti_2 sites. Improved agreement can be obtained by assuming that a fraction $c_3(\mu_{\min})$ of the $NiTi_3$ sites are filled initially, which introduces $1-c_3(\mu_{\min})$ as another parameter into Eq. (3.13). In any case, the Ni-Ti behavior, while not definitive, is consistent with the overall factor of 1.9 hydrogen atoms per metal atom in each type of site.

We next consider the Cu-Ti system, which, to our knowledge, is the only other glass in which hydrogen-content studies have been carried out over a wide range of compositions. From simple averaging estimates, we expect Cu-Ti to behave similarly to Ni-Ti or Pd-Ti and store hydrogen in Ti_4, $CuTi_3$, and possibly some fraction of the Cu_2Ti_2 sites. The *total* hydrogen content should then be given by

$$H/M=1.9[x^4+4x^3(1-x)+6x^2(1-x)^2c_2(\mu)] \tag{3.14}$$

with an appropriate x-independent choice of $c_2(\mu)$. In Table II we compare the data of Maeland *et al.*[3] obtained at $P=1$ atm, $T=295$ K ($\mu=-38.5$ kJ/mol) to Eq. (3.14). Since we do not have a "universal curve" for Cu-Ti, we *fit* $c_2(\mu)=0.22$ to obtain the experimental H/M at the *single* composition $x=0.35$ and find *excellent agreement over the full range of* x. Interestingly, the hydrogen content of Cu-Ti obtained by Hwang *et al.*[4] under apparently very different conditions of $P=50$ atm, $T=403$ K is nearly identical to that of Maeland *et al.* This is now clearly understood, however, by simply noting that $\mu=-43.0$ kJ/mol under these conditions, which is extremely close to the μ of Maeland *et al.*

Finally, a number of studies on other ETM/LTM glasses at isolated compositions have been made. Simple

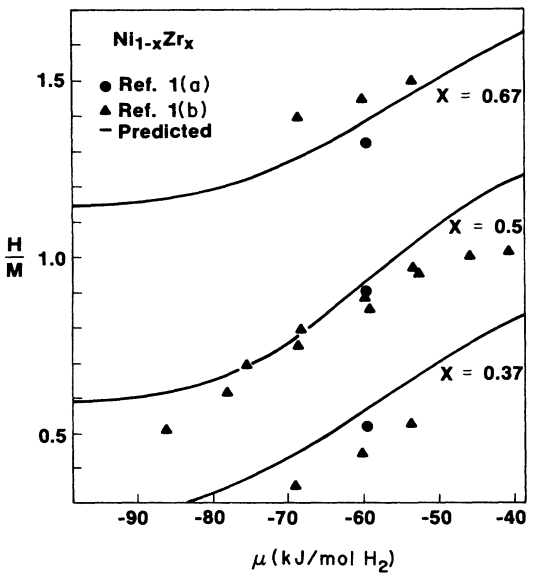

FIG. 5. Hydrogen-to-metal ratio H/M in $Ni_{1-x}Zr_x$ vs hydrogen chemical potential μ as predicted (——) and obtained experimentally [▲, Ref. 1(b), ●, Ref. 1(a)] at various compositions x. The experimental data spans a wide range of temperature (373–573 K) and pressure (0.1–50 atm) and the predicted H/M is obtained as described in Fig. 4 and the text.

TABLE II. Comparison of predicted $H/M=1.9[x^4+4x^3(1-x)+6x^2(1-x)^2c_2(\mu_{\max})]$ and experimental values of Maeland *et al.*[3] for Cu-Ti at 293 K, $P=1$ atm. $c_2(\mu_{\max})$ is fit to experiment at $x=0.35$. Also shown is data on Cu-Ti obtained by Hwang *et al.* (Ref. 4) at 403 K. $P=50$ atm., which has very nearly the same $\mu_{\max}$.

	H/M for $Cu_{1-x}Ti_x$		
X	Maeland *et al.*	Predicted	Hwang *et al.*
0.35	0.37	0.37 (fit)	0.42
0.50	0.68	0.75	0.69
0.60	0.96	1.04	
0.65	1.15	1.19	1.23

averaging suggest that none of the ETM/LTM glasses (ETM is Ti, Zr, Hf) studied to data store hydrogen in A_3B ($n=1$) sites. Therefore, we predict that the maximum obtainable H/M values are *bounded above* by the value of $H/M=1.9[x^4+4x^3(1-x)+6x^2(1-x)^2]$ (i.e., full occupation of the $n=4$, 3, and 2 sites). Figure 6 presents a compilation of the maximum H/M values we have found for a variety of systems over a wide range of composition, and we observe that the bound is quite accurate. Those systems which are far below the bound (such as Cu-Ti and Pd-Ti) store very little or no hydrogen in the A_2B_2 sites.

We have presented many measurements, both ours and those of other workers, which confirm that an effective number of about 1.9 hydrogens per metal atom is an upper limit to *total* hydrogen storage in this class of glassy alloys. Moreover, the $N_{\text{eff}}=1.9$ holds also as the prefactor for the hydrogen content in each type of tetrahedral site in these materials. This observation has several profound consequences on the nature of these glasses. The persistence of a composition and alloy independent N_{eff} implies that these glasses are all structurally similar, the basic local structure of tetrahedral units being very similar in all cases. The universal behavior of the chemical potential is also an indication of the structural similarity with changing composition and its successful application at different temperatures is an indication of the dominance of energy over entropy in the hydrogen free energy. The comparisons often made between hydrogen capacities of crystalline and amorphous alloys at the same composition in attempts to understand the glass behavior are seen to be largely irrelevant. We will discuss some of these points further in Sec. V.

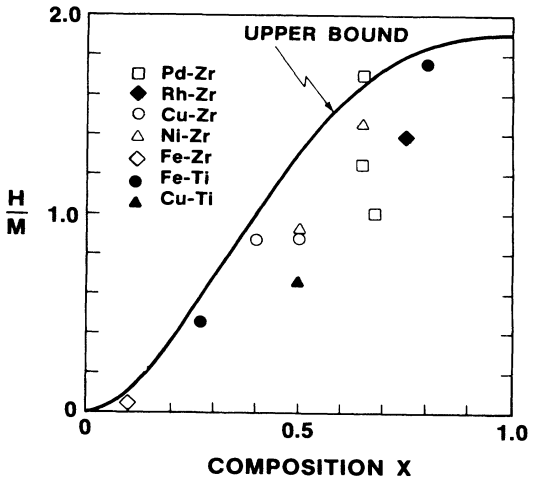

FIG. 6. Predicted upper bound for total hydrogen content in ETM/LTM amorphous alloys $H/M=1.9[x^4+4x^3(1-x)+6x^2(1-x)^2]$, and maximum experimental H/M for various ETM/LTM glasses at isolated ETM compositions x. The upper bound is accurate for all of these glasses: Pd-Zr (Refs. 5 and 19), Rh-Zr (Ref. 5), Cu-Zr (Ref. 6), Ni-Zr (Ref. 9), Fe-Zr (Ref. 20), Fe-Ti (Refs. 7 and 21), Cu-Ti (Ref. 8). The more comprehensive data presented in Figs. 3 and 4 and Table II is not included here.

IV. NEAR-NEIGHBOR BLOCKING: ORIGIN OF THE x AND SITE-INDEPENDENT $N_{\text{eff}}=1.9$

We have provided considerable experimental verification of the limiting value of 1.9 hydrogens per metal in ETM/LTM transition metal glasses. However, as recognized by Samwer and Johnson,[5] the total number of interstitial sites available for hydrogen storage in crystalline materials and glass models is in the range of $N=5-6$ sites per metal atom, all of which may be considered as basically (distorted) tetrahedral sites. Crystalline materials also exhibit "reduced" hydrogen capacities, and it has been necessary to introduce very strong short-ranged repulsive interactions between interstitial hydrogens to limit the total occupation of sites to some fraction of the total number of available sites.[22] The origin of the repulsive interaction is electronic in nature and, being much larger than other relevant energies in the hydrides, is often assumed to be infinite out to first, second, or even third neighbor distances. The range of the interactions has been specified as 2.1 Å independent of material by Switendick.[14] Accordingly, we adopt the assumption of infinite (at least 200 kJ/mol) *near-neighbor* hydrogen-hydrogen interactions in the glassy alloys.[23] Thus, no two interstitial sites sharing a common triangular face of a tetrahedron (i.e., having three common metal atom neighbors) may be simultaneously occupied by hydrogens, an exclusion referred to as "blocking."

Blocking interactions immediately imply that site-site *correlations* are important. For example, the amount of hydrogen that can be stored in the A_2B_2 sites in a chemically random $A_{1-x}B_x$ alloy now depends not only on the number of A_2B_2 sites [$\sim x^2(1-x)^2$] but also on the types and occupations of the sites neighboring a typical A_2B_2. Such correlations should destroy the direct and simple relation between hydrogen occupation of a particular type of site n and the number of those sites occurring in a chemically random alloy [as described by Eq. (3.8)]. Thus in principle, the quantity α appearing in Eqs. (3.8) and (3.9) should depend on both site type n and composition x. We therefore generalize Eq. (3.8) and introduce the fractional occupation factors $\alpha_n(x)$, defined so that the maximum occupation of the type-n sites is

$$\Delta H/M\mid_{\max}=N\alpha_n(x)\binom{4}{n}x^n(1-x)^{4-n}\ . \tag{4.1}$$

$\alpha_n(x)$ measures the deviation in the maximum occupation of the type-n sites from the total number of type-n sites available. The surprising experimental observation is that $N\alpha_n(x)=1.9$. The occupation fractions are not only each independent of x but take on the same value of $\alpha=0.34-0.38$. We will show that near-neighbor blocking does in fact lead to a nearly x-independent fraction $\alpha_4(x)\approx\alpha_3(x)\approx\alpha_2(x)\approx\alpha$, so that Eq. (3.8) is valid. The precise numerical value of α does depend on structure but its insensitivity to composition is less structure dependent. Below, we demonstrate that a structure based on *fivefold rings of tetrahedral interstitial sites* predicts $\alpha\approx\frac{3}{8}$ and $N\alpha=1.9-2.1$, in excellent agreement with our experiments. In contrast, structures consisting

TABLE III. Number of $A_{4-n'}B_{n'}$, interstitial sites neighboring a $A_{4-n}B_n$ site in a chemically random $A_{1-x}B_x$ alloy.

Neighbor site	Site type $A_{4-n}B_n$		
$A_{4-n'}B_{n'}$	B_4	AB_3	A_2B_2
B_4	$4x$	x	
AB_3	$4(1-x)$	$1+2x$	$2x$
A_2B_2		$3(1-x)$	2
A_3B			$2(1-x)$

of evenfold rings yield $\alpha \approx 0.45-0.5$ and $N\alpha \gtrsim 2.5$, in some disagreement with our results.

To understand how the $\alpha_n(x)$ cannot only be x independent but also take on a similar n-independent value, it is important to recognize that correlations exist between the interstitial sites of a chemically random alloy. Although the A and B metal atoms are randomly distributed, each metal atom influences the type of its many (more than 20) neighboring interstitial sites. The identities of interstitial sites sharing any metal atoms in common are thus related. Table III shows the number of $A_{4-n'}B_{n'}$, sites neighboring a typical $A_{4-n}B_n$ site as a function of overall alloy composition x. As illustrated in this table, both AB_3 and A_2B_2 sites *have on average at least one neighbor of the same type* over the full range of compositions. Therefore at most one out of every two of these sites can be occupied in the presence of blocking, even at low x where very few AB_3 and A_2B_2 sites occur. In addition, sites differing by more than one A or B atom are never near neighbors, leading to some decoupling of the occupation fractions α_n. These points only depend on the *local* tetrahedrally coordinated interstitial structure of the random alloy, whether crystalline or amorphous.

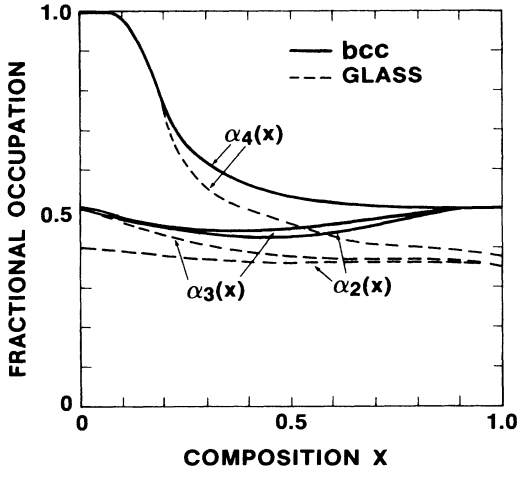

FIG. 7. Maximum fractional occupations $\alpha_n(x)$ of the $A_{4-n}B_n$ tetrahedral sites in the $A_{1-x}B_x$ random alloy with infinite near-neighbor hydrogen-hydrogen interactions (blocking) as a function of alloy composition x: (——) bcc, (— — —) glass. Note the similar values of the $\alpha_n(x)$ for different n over a wide range of x, $\alpha_n(x)=0.45-0.5$ for bcc and $\alpha_n(x)\approx\frac{3}{8}$ for the glass.

To elucidate the detailed effects of blocking as a function of composition x, we proceed as follows. In the next subsection, we analyze the occupation fractions $\alpha_n(x)$ of a tractable model, the bcc random alloy, and show that the $\alpha_n(x)$ are insensitive to composition over a wide range of x (see Fig. 7). The actual values of $\alpha_n(x)=0.45-0.5$ we obtain are structure dependent and of secondary importance. In Sec. IV B, we discuss the more complicated case of the $\alpha_n(x)$ expected in a model amorphous alloy based on icosahedral structural units. Because of the *fivefold rings* in this structure, the typical values of the $\alpha_n(x)$ are in the range of 0.35–0.4, comparable to those determined experimentally.

A. Blocking in a random bcc lattice

The interstitial sites of a bcc lattice are tetrahedrally coordinated and each has four neighboring metal atoms defining its site type, as shown in Fig. 8. Thus the bcc structure has a local topology identical to our picture of the glass as discussed in Sec. III. The features of the occupation fractions $\alpha_n(x)$ in the bcc case are much easier to determine than in the glass and will guide us in studying the more complicated amorphous structure. We consider near-neighbor blocking only; our study is therefore *not* relevant for real bcc materials such as Nb, for which blocking out to third neighbors is necessary to obtain agreement with experimentally measured Nb-H phase diagrams. In the bcc alloy, we are interested primarily in the variations of $\alpha_n(x)$ with x and n. Since a chemically random $A_{1-x}B_x$ bcc alloy differs from a chemically random glass in the structure at further neighbors, consisting of fourfold and sixfold rings of interstitial sites in constrast to the fivefold rings which predominate in many models of the glassy state, the typical values of $\alpha_n(x)$ calculated here may (and in fact do)

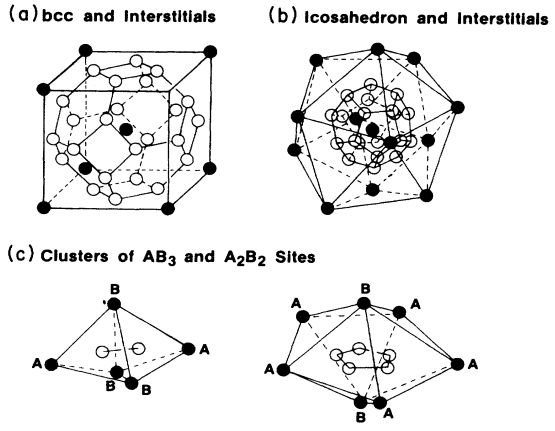

FIG 8. (a) Interstitial sites of the bcc lattice. Note the occurrence of fourfold and sixfold ring of interstitial sites. (b) Icosahedron (the assumed local structure of the glass) and its interstitials, which form a dodecahedra consisting of fivefold rings of interstitial sites. (c) Clusters of AB_3 and A_2B_2 sites in the low-x limit of the glassy alloy.

differ from those we will estimate for the glass. Keep in mind, however, that our real goal in this exercise is to determine the sensitivity of $\alpha_n(x)$ to n and x. We first determine the exact high and low x limits of the $\alpha_n(x)$.

Low x limit. At low x, all B_4 sites may be filled since each has only higher energy AB_3 neighbors. Hence, $\alpha_4(x=0)=1$. The AB_3 sites always have one AB_3 neighbor, so that one of the two may be occupied and thus $\alpha_3(x=0)=\frac{1}{2}$. The A_2B_2 sites, while each having two A_2B_2 neighbors (see Table III), actually form fourfold or sixfold rings, within which two or three sites may be occupied, respectively, yielding $\alpha_2(x=0)=\frac{1}{2}$. Note that $\alpha_3=\alpha_2$ in this limit.

High x limit. At $x=1$, all interstitial sites are B_4 and blocking restricts the maximum occupation to a sublattice of every other site, so that $\alpha_4(x=1)=\frac{1}{2}$. When an A atom is introduced into the alloy, a cluster of 24 AB_3 interstitial sites is created. Preferential occupation of the lower energy B_4 sites which surround this "defect," at the expense of low occupation of the (higher energy) AB_3 sites, does not occur because the B_4 boundary sites are neighbors of each other. Therefore, exactly $\frac{1}{2}$ of the AB_3 sites may be filled and in precisely the manner that these sites would be filled if the "defect" were not present. Hence, $\alpha_3(x=1)=\frac{1}{2}$. Finally, if a pair of neighboring A atoms are introduced into the all B alloy, either 4 A_2B_2 and 40 AB_3 or 6 A_2B_2 and 36 AB_3 sites are created. Again, relaxation of the occupations around the defect does not increase the total B_4 or AB_3 occupations and so exactly $\frac{1}{2}$ of the A_2B_2 sites may also be filled: $\alpha_2(x=1)=\frac{1}{2}$. Note that $\alpha_4=\alpha_3=\alpha_2=\frac{1}{2}$ in this limit, which is identical to the values of α_3 and α_2 in the low-x limit.

To determine the behavior in between the *exact* low- and high-x limits determined above, we have carried out static computer simulations of hydrogen filling with blocking interactions on a $(20)^3$ unit cell random $A_{1-x}B_x$ bcc lattice ($\sim 10^5$ interstitial sites) as a function of x. The details are discussed in the Appendix. The results for $\alpha_4(x)$, $\alpha_3(x)$, and $\alpha_2(x)$ versus x are shown in Fig. 7. The exact high- and low-x limits are obtained (precisely because we *know* these limits and are able to construct a filling sequence which correctly yields them; see the Appendix), along with the correct initial slopes at both limits and the slow variation in total occupation on decreasing x from 1. Deviations from the limiting value of $\frac{1}{2}$ are small [the minimum value obtained is $\alpha_2(x=0.5)\approx 0.43$] and $\alpha_3(x)$ and $\alpha_2(x)$ track one another quite closely over the entire range of x. Also, we find $\alpha_4(x)\approx\frac{1}{2}$ down to $x=0.5$. Below $x=0.5$, the number of B_4 sites decreases so rapidly (like x^4) that the deviations in $\alpha_4(x)$ in this region give inconsequential corrections to the total H/M. Since the $\alpha_n(x)$ are nearly independent of x and n (in the composition range where they contribute significantly to the total H/M), the maximum occupations of the type-n sites follow the random statistics quite closely but with a prefactor reduced by ~ 0.45–0.5 relative to the total number of these sites. For the bcc alloy, the hydrogen content in each type of site is well approximated by

$$\Delta H/M\mid_{\max}\approx 0.5N\begin{bmatrix}4\\ n\end{bmatrix}x^n(1-x)^{4-n}$$

over nearly the entire range of compositions. To reiterate the point of this example, the $\alpha_n(x)$ are insensitive to composition in the composition range where they are important in determining H/M, while the particular structure of the bcc lattice results in typical values of $\alpha_n=0.45$–0.5 for $n=4,3,2$.

B. Blocking in an amorphous alloy

We consider the glassy state to be characterized by tetrahedral packing and tetrahedral interstitial sites. While computer models of the relaxed random close-packed structure show 86% of the interstitial sites to be tetrahedral, they contain high fractions (25%) of both fourfold and sixfold rings. Other recent glass models, on the other hand, characterize the glass as consisting predominantly (90%) of fivefold rings, with the residual rings being higher coordinated sixfold rings.[24] The dominance of fivefold rings is also present in the topologically close-packed Frank-Kasper phases, and Nelson[25] has suggested that the "ideal" glass corresponds to a Frank-Kasper phase with an infinite unit cell. We assume fivefold rings are the main structural feature in glasses and are then naturally led to the icosahedron as a basic building block. While the higher-coordinated CN14, CN15, and CN16 Kasper polyhedra (containing 2, 3, and 4 sixfold rings, respectively, in addition to 12 fivefold rings) must be present to relieve frustration arising in the packing of icosahedra, we focus here on the fivefold rings only and hence on icosadedra. In the Appendix we discuss simulation results on a chemically random $A_{1-x}B_x$ alloy of the $MgCu_2$ Laves structure (a Frank-Kasper phase) which support the conclusions reached below using icosahedra only.

Because of the fivefold rings, there is frustration in the filling of the interstitial sites of a single icosahedron in the presence of near-neighbor blocking interactions. Specifically, the interstitial sites of an icosahedron lie at the vertices of a dodecahedron (20 vertices) and 12 fivefold pentagonal rings of interstitial sites form the faces of the dodecahedron (see Fig. 8). With near-neighbor blocking, only two occupied sites out of any five-ring are allowed and the maximum occupation is limited to $\frac{8}{20}=0.4$. As an aside, the maximum occupations of CN14, CN15, and CN16 polyhedra are also about 0.4 ($\frac{3}{8}$, $\frac{11}{26}$, and $\frac{3}{7}$, respectively) because of the high fraction of fivefold rings. Additional frustration occurs in occupying the sites of packed dodecahedra consisting of a central unit surrounded by 12 slightly distorted units, each sharing a pentagonal face with the central unit. In this case, occasional singly-occupied five-rings are necessary (dodecahedra with only $\frac{7}{20}=0.35$ occupation). The maximum fractional occupation is thus limited to $\approx\frac{3}{8}$, which is somewhat lower than the value of $\frac{1}{2}$ obtained for the bcc crystal. We now consider the individual occupation fractions $\alpha_n(x)$ of the B_4, AB_3, and A_2B_2 sites in the limits of low and high x. It is important to obtain these

limits explicitly because static simulation studies are not completely reliable, especially at high x (see the Appendix).

Low x limit. Here, the B_4 sites and AB_3 sites occur just as they do in the bcc alloy, in "clusters" of 1 and 2, respectively. Thus, $\alpha_4(x=0)=1$ and $\alpha_3(x=0)=\frac{1}{2}$. The A_2B_2 site clusters differ from those in the bcc crystal, appearing now in fivefold rings, of which only two sites may be occupied, giving $\alpha_2(x=0)=0.4$.

High x limit. The above discussion of the occupation of packed icosahedra corresponds precisely to the B_4 occupation at $x=1$ and so $\alpha_4(x=1)\approx\frac{3}{8}$. Introducing a single A atom into the center of an icosahedron creates a cluster of 20 AB_3 interstitial sites. While zero AB_3 occupation and full occupation of the 20 B_4 boundary sites is possible, the resultant blocking of next-neighbor B_4 sites leads to nearly the same total occupation of the B_4 sites. The most favorable configuration (minimizing the grand potential when $\mu \gg E_3$) is obtained by filling $\alpha_3(x=1)=\frac{7}{20}=0.35$ of the AB_3 sites, as if the A atom replaces a B atom at the center of a low ($\frac{7}{20}$) occupation dodecahedron, with no relaxation of the hydrogen configuration. The insertion of the "defect" AB_3 sites at high x in the amorphous alloy is thus very similar to that in the crystalline alloy. Introducing a pair of neighboring A atoms into the otherwise all B glass generates 5 A_2B_2 sites in a five ring, surrounded by 30 AB_3 sites which are, in turn, surrounded by B_4 sites. Determining the optimal occupation in this case is quite difficult because of the size of the defect and hence $\alpha_2(x=1)$ is the only limiting quantity which cannot be obtained with certainty. Clusters extending out to the near-neighbor dodecadra of the central pair of dodecahedra have been studied that contain the central 5 A_2B_2 and 30 AB_3 sites along with 140 B_4 sites. The constraint of $\frac{2}{5}$ occupation of the outermost faces of the near-neighbor dodecahedra (60 B_4 sites) has been imposed and represents the beginning of bulk, or "defect-free" occupation. A maximal B_4 occupation was obtained by filling *none* of the A_2B_2 sites, the 10 AB_3 neighbors of the A_2B_2 sites and $\frac{30}{80}$ of the remaining B_4 sites. However, a "random" configuration attained 2 A_2B_2 sites, 10 AB_3 sites and $\frac{29}{80}B_4$ sites, marginally different from the highly ordered structure. At small $1-x$ the overlap of large A_2B_2 defect regions should tend to favor the flexible "random" configuration over the highly ordered structure and so it is reasonable to postulate that the random configuration result of $\alpha_2(x \lesssim 1)\sim 0.4$ quickly becomes accurate with decreasing x. Note that as in the bcc alloy, the limiting values of the $\alpha_n(x)$ are very similar.

In the intermediate x regime, the detailed ring structure is less important: the differences between the random alloy bcc lattice and glass are not as striking as at high and low compositions since full rings of a single type of site are unlikely. The occupation fractions $\alpha_n(x)$ in the intermediate range of compositions are therefore not expected to vary dramatically. In fact, $d\alpha_3/dx$ and $d\alpha_4/dx$ at low x are the same in both bcc and glass, with $d\alpha_2/dx$ being only slightly different in the two cases. In addition, the interplay between the occupations of different site types is similar to that which occurs in the bcc random alloy and leads to approximately x-independent occupation fractions. That is, on decreasing x from 1, the increasing fractional occupation of the B_4 sites decreases the occupation of the AB_3 sites neighboring the B_4 sites, and the lower AB_3 occupation then allows comparatively more A_2B_2 sites to be occupied. Simulated fillings of the interstitial sites of a $A_{1-x}B_x$ alloy having the $MgCu_2$ Laves structure show these same qualitative features and weakly x-dependent $\alpha_n(x)$ [as noted in the Appendix, however, detailed comparisons are not warranted because of difficulties in obtaining the proper $\alpha_n(x)$ at high x via simulation]. In Fig. 7 we show the variations in the occupation factors $\alpha_4(x)$, $\alpha_3(x)$, and $\alpha_2(x)$ with x expected for our model of the glass structure. Over the range of x that any type of site contributes appreciably to the total hydrogen occupation (B_4, $0.5<x<1$; AB_3, $0.25<x<1$; A_2B_2, $0<x<0.8$), the *fractional occupations are nearly the same, x-independent factor of* $\alpha=\frac{3}{8}$ *for all occupiable sites.*

C. Summary

The maximum fractions of occupiable sites in the ETM/LTM glasses have been demonstrated to be $\alpha_4(x)\approx\alpha_3(x)\approx\alpha_2(x)\approx\frac{3}{8}$, nearly independent of composition. The number of interstitial sites per metal atom N is not known precisely, but for icosahedral packing, the relaxed Bernal model and a number of Frank-Kasper phases, N is in the range of $N=5-5.6$ sites per metal atom. Therefore, we predict that Eq. (3.8) is valid with the *effective* number of occupiable sites N_{eff} in these alloy glasses being

$$N_{\text{eff}}=N\alpha\approx 1.9-2.1\ , \tag{4.2}$$

which is in excellent agreement with the experimentally derived value of $N_{\text{eff}}=1.9$. In Fig. 9, we present

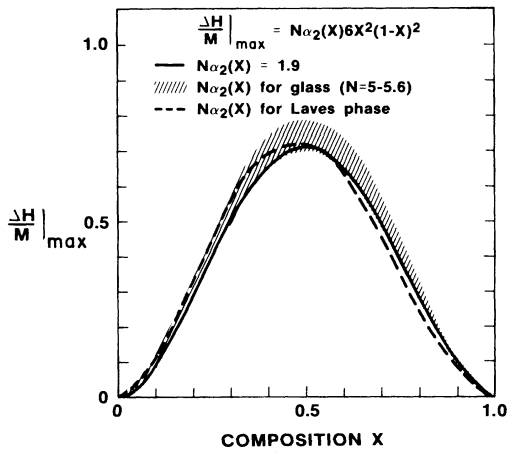

FIG. 9. Maximum hydrogen storage $\Delta H/M\,|_{\max} = N\alpha_2(x)(\frac{4}{2})x^2(1-x)^2$ in the A_2B_2 tetrahedral sites as derived experimentally (solid line) and predicted for the glass (shaded region) and $MgCu_2$ Laves structure (dashed line).

$$\Delta H/M\mid_{\max}=N\alpha_2(x)\begin{bmatrix}4\\2\end{bmatrix}x^2(1-x)^2$$

using the $N\alpha_2(x)$ as derived experimentally and as obtained from our considerations of the glass and Laves structures. Figure 9 is indicative of both the generally good agreement between experiment and theory and of the insensitivity of $\Delta H/M\mid_{\max}$ to the slow variations in $\alpha_n(x)$, which are masked by the more rapidly varying $x^n(1-x)^{4-n}$ factor.

The main ingredient of the glass model which yields the correct fractions of occupiable sites is the assumed predominance of fivefold rings of tetrahedra, and hence fivefold rings of interstitial sites.[25,26] If the glass consisted of even numbered rings, as is the case in the bcc alloy, the limiting occupations would be approximately $\alpha\approx\frac{1}{2}$ rather than $\alpha\sim 0.4$, leading to $N_{\text{eff}}>2.5$, which is somewhat larger than observed. While frustation effects lower this number slightly, as they do in our model of the glass, a predominance of even numbered rings in the glass could not lead to the observed limiting hydrogen-to-metal ratio. We note that the second-neighbor blocking in both the crystal and glass limits the total occupations to *much smaller* fractions than seen experimentally. Thus, even rings and second-neighbor blocking are not able to reproduce the observed occupations.

V. DISCUSSION

We have taken a few simple ideas suggested by experiment (chemically random alloys, tetrahedral interstitials of distinct chemical compositions $A_{4-n}B_n$, and sequential occupation of sites according to ETM atom coordination) and combined them with near-neighbor blocking and a structure based on fivefold rings to predict that the three quantities $\alpha_4(x)$, $\alpha_3(x)$, and $\alpha_2(x)$ are essentially independent of x and take on a common value of $\approx\frac{3}{8}$. This is in close agreement with experiment. While the necessity of blocking comes as no surprise, being required to understand hydrogen storage in crystalline materials, the resultant general insensitivity of the $\alpha_n(x)$ to n and x and the particular necessity of fivefold rings in the glass to obtain quantitative agreement with experiment are very interesting results. The predominance of fivefold rings is consistent with the work of Steinhardt *et al.*[26] which indicates strong icosahedral bond order in supercooled Lennard-Jones liquids and relaxed "amorphon" models. It is also consistent with disclination models of the glassy state[25] in which the average number of tetrahedra surrounding any bond (near-neighbor pair of metal atoms) is only slightly greater than 5 [compare to Fig. 8(c)]. As remarked earlier, random close-packed structures are composed mainly of tetrahedral units,[16] but do not exhibit strong icosahedral order[26] and contain many fourfold and sixfold rings. Such models could possibly yield hydrogen occupation characteristics similar to those observed here, but this may only be tested by *dynamic* simulations (to allow for relaxation) of hydrogen in structures suitably decorated to represent a binary glass. Unfortunately, even for the static simulations described in the Appendix, a large total number of sites is required to obtain good statistics for each type of site and so dynamic simulations may be effectively precluded.

The existence of the composition and alloy-independent $N_{\text{eff}}=1.9$ has an important consequence also. That is, whatever structure is consistent with this N_{eff}, that structure is the same for all the ETM/LTM glasses discussed here. This isomorphism (at least as seen by interstitial hydrogens) implies that varying chemical effects such as heats of mixing and varying atomic sizes of the A and B atoms has little consequence, at least for $A=$Ni, Pd, Cu and $B=$Ti, Zr. Since these two aspects are considered to govern the chemical and structural order of glasses, the apparent isomorphism is intriguing. Studies of a wider range of ETM/LTM glasses (e.g., larger atomic size differences) should be carried out to ascertain the extent of this isomorphism.

In this paper we have not addressed any of the theoretical aspects associated with *predicting* the universal curve shown in Fig. 1. We have used a simple picture of a bare hydrogen density of states which may be decomposed into distinct contributions from different tetrahedral sites in the glass. The inclusion of blocking effects to limit the maximum fractional occupations of each type of site to $\alpha\approx\frac{3}{8}$ has been discussed without considering the effects of blocking on the measured chemical potential. Clearly, a full statistical mechanical treatment including blocking would yield not only the maximum fractional occupations but also the chemical potential as a function of hydrogen concentration. The universal curve of Fig. 1 suggests that filling of the A_2B_2 sites occurs in an x-independent manner. However, at high x these sites are blocked out mainly by surrounding occupied AB_3 sites while at low x the A_2B_2 sites are in isolated clusters and block out each other. The behavior of the chemical potential versus hydrogen concentration within a site type is therefore in principle a function of alloy composition. In a subsequent paper,[27] we will address this point and show that the predicted shape of μ versus $\Delta H/M$ is remarkably *insensitive* to composition. In fact, μ versus $(\Delta H/M)/(\Delta H/M\mid_{\max})$ may be well approximated by a bare density of states *renormalized* by a factor of $\approx\frac{3}{8}$, which is essentially the approximation used in the present work. We will also examine the widths σ_n of the bare DOS which are obtained from a proper analysis of the experimental measurements, the role of further-neighbor hydrogen-hydrogen interactions (due to elastic effects) in modifying the predicted chemical potential as a function of H/M, and comment on the possibility of observing phase transitions in these systems (see Ref. 17).

To conclude, we reiterate our main findings and hence answer all of the question raised in the Introduction.

1. The proportionality of the hydrogen content to $\binom{4}{n}x^n(1-x)^{4-n}$ implies that the interstitial sites for hydrogen are tetrahedral and that these glasses are chemically random alloys.

2. Ni-Zr and many other glasses (Ni-Ti, Cu-Ti, for example) store some hydrogen in A_2B_2 tetrahedral sites as well as AB_3 and B_4 sites under standard conditions.

3. The chemical potential versus concentration, indicative of the manner in which sites of a given type are filled, is independent of composition.

4. The composition, alloy, and site-type independent proportionality factor of 1.9 implies that these glasses are isomorphic, i.e., that there is little variation in the structure at least to second neighbors, from alloy to alloy, over a range of compositions within a single alloy, or with preparation technique.

Furthermore, agreement between our theoretical and experimental occupations leads us to conclude that (1) near-neighbor blocking exists between hydrogen atoms in the glass and this restricts the fraction of occupiable hydrogen sites of each type to $\approx\frac{3}{8}$, giving a maximum $H/M=1.9$ in these alloys; (2) hydrogen storage data is consistent with a glass structure composed mainly of fivefold rings of tetrahedra, and therefore, fivefold rings of interstitial sites.

We have found that hydrogen can be used as a probe of the local structure of glassy alloys and that the simplest picture of a chemically random glass which exhibits local icosahedral order (or at least fivefold rings of tetrahedra) appears to be consistent with measurements of hydrogen in these glasses. In addition, the structure of sputtered and rapid-quenched materials is evidently the same for these alloys. The measurement of hydrogen capacities and occupation statistics of amorphous alloys produced by other methods, such as mechanical alloying,[28] or after annealing should provide further insight into this possibility of simple, universal structure in ETM/LTM glasses.

ACKNOWLEDGMENTS

We would like to thank Dr. H. Scher and Dr. L. Turkevich for stimulating discussions during the course of this work.

APPENDIX

In this appendix, we briefly discuss some details of our static simulations of hydrogen occupation in the bcc $A_{1-x}B_x$ alloy. We then present and discuss results of a similar study in a $A_{1-x}B_x$ chemically random alloy in which A and B occupy the metal atom sites of the $MgCu_2$ Laves structure (a Frank-Kasper phase). The $MgCu_2$ Laves phase, consisting of icosahedra and CN16 polyhedra, contains primarily fivefold rings in a large (24 atoms) unit cell and therefore contains a key feature of the glass structure we advocate here. As we shall see, however, static simulations are not adequate over the full range of alloy compositions x for this structure and our results on the Laves phase lend only qualitative support to the arguments given in the main text.

In general, we are interested in the maximum fractional occupations $\alpha_n(x)$ of each type of site ($n=4,3,2$) as a function of composition x. From a thermodynamic viewpoint, $\alpha_n(x)$ corresponds to the fraction of type-n sites occupied at a chemical potential μ that is above the typical energies of the type-n sites, i.e., $\mu>E_n+\sigma_n$. If the energies of all the type-n sites are well below μ, the distribution of type-n site energies is unimportant, and we may simply assign all type-n sites the same energy E_n and set $\sigma_n=0$. For a given realization of the chemically random alloy (A and B atoms distributed randomly on the sites of the lattice), the B_4 sites (lowest in energy) are then filled first, subject to near-neighbor blocking. After the B_4 sites are maximally occupied, the AB_3 sites are then maximally occupied, followed by the A_2B_2 sites. Once a site is occupied, it remains occupied for the remainder of the simulation. For such a static simulation, sites of the same type (e.g., B_4) are *not* selected from the lattice and filled at random because this introduces artificial *frustration* that would be relieved in a dynamic simulation. Instead, sites are occupied in a sequential fashion. Labelling the origin of each unit cell by coordinates (i,j,k), all occupiable sites within unit cell (i,j,k) are filled and then the neighboring unit cell $(i+1,j,k)$ is considered, just as one would fill the elements of a $3d$ array. Sites within each unit cell must also be filled in a manner such that the entire filling procedure yields the correct fractional occupations at $x=1$. In the bcc structure, each unit cell is constructed to contain two six-rings, each of which is filled cyclically thereby guaranteeing that the correct fractions $\alpha_n(x=1)=\frac{1}{2}$ are obtained. In contrast, random selection and filling of sites in the bcc structure gives a fractional occupation of only about 0.37 at $x=1$. The random selection is actually equivalent to having a distribution of site energies ($\sigma_n>0$) and occupying sites starting with the lowest energy site but not allowing for any subsequent relaxation of the occupations. Such a procedure does not minimize the grand potential of the system at near-maximum fillings ($\mu>E_n+\sigma_n$) because relaxations are important to relieve frustration and permit higher occupations. It is thermodynamically preferable to fill sites in the sequential manner described above. The thermodynamics of this problem is discussed in some detail in Ref. 27.

The $MgCu_2$ Laves structure contains 24 metal atoms and 136 tetrahedral interstitial sites per unit cell ($N=5.666$), with each metal atom at the center of an icosahedron or a CN16 polyhedron.[29] A simulation study of the hydrogen occupations in a $A_{1-x}B_x$ alloy having this structure first requires knowledge of the near-neighbor metal atoms (to determine the site type) and the near-neighbor interstitial sites of all 136 sites. Making use of the Fd3m symmetry of the structure and the known symmetries and coordinates of the metal atoms and interstitial sites,[29,30] this information may be obtained in a systematic manner. The simulated filling then proceeds unit cell by unit cell as described above. However, it proves difficult to devise a filling sequence within each unit cell which maximizes the hydrogen occupation. We have obtained the highest occupations by cyclically filling all the six rings in each unit cell first and then sweeping again through the lattice to fill all the remaining sites in each unit cell. The occupation fraction $\alpha_4(x=1)=0.35$ obtained is still slightly lower than the expected value of $\alpha_4(x=1)\geq\frac{3}{8}$ (since the structure consists of icosahedra and CN16 polyhedra), indicating a small amount of artifical frustration. Also, the values $\alpha_3=0.29$ and $\alpha_2=0.27$ obtained in this $x=1$ limit are not correct and are probably also too low by small

amounts. At low x (few B atoms), however, very few sites in each unit cell are occupiable and our filling sequence does not introduce frustration. We thus find the correct low-x limits of $\alpha_4(x=0)=1$, $\alpha_3(x=0)=\frac{1}{2}$, and $\alpha_2(x=0)\sim 0.4$. With increasing x, the behavior of the $\alpha_n(x)$ are very similar to the bcc and postulated glass results shown in Fig. 7. The static simulations on the Laves structure are thus reliable at low x but are in some error at higher x. The variations of the $\alpha_n(x)$ with x between $x=0$ and $x=1$ are smooth (and nearly linear in x for $x>0.5$), giving no indication of the range of x in which frustration begins to play an important role. Despite the inaccuracies at high x ($x>0.5$?), the variations in the $\alpha_n(x)$ are still not too severe, as indicated by the similarity between $N\alpha_2(x)(\frac{4}{2})x^2(1-x)^2$ with $\alpha_2(x)$ as determined here for the Laves phase (with $N=5.666$) and with $N\alpha_2(x)=1.9$ as derived experimentally (see Fig. 9). In conclusion, static simulation results on the $MgCu_2$ Laves phase structure are qualitatively similar to the bcc results and support the conjecture of slowly varying $\alpha_n(x)$ in the glass but cannot be used reliably to predict the hydrogen occupations in the glass structure over the full range of compositions.

[1](a) K. Aoki, A. Horata, and T. Masumoto, in *Proceedings of the 4th International Conference on Rapidly Quenched Metals,* edited by T. Masumoto and K. Suzuki (Japan Institute of Metals, Sendai, 1982), p. 1649; (b) K. Aoki, M. Kamachi, and T. Masumoto, J. Non-Cryst. Solids **61/62**, 679 (1984).

[2]E. Batalla, Z. Altounian, D. B. Boothroyd, R. Harris, and J. O. Strom-Olsen, in *Hydrogen in Disordered and Amorphous Solids,* edited by G. Bambakidis and R. C. Bowman, Jr. (Plenum, New York, 1986).

[3]A. J. Maeland, L. E. Tanner, and G. G. Libowitz, J. Less-Common Met. **74**, 279 (1980).

[4]C. H. Hwang, S. Kang, K. Cho, and K. Kawamura, Scr. Metall. **20**, 1231 (1986).

[5]K. Samwer and W. L. Johnson, Phys. Rev. B **28**, 2907 (1983).

[6]K. Dini and R. A. Dunlap, J. Phys. F **15**, 273 (1985).

[7]A. J. Maeland, in *Hydrogen in Disordered and Amorphous Solids,* edited by G. Bambakidis and R. C. Bowman, Jr. (Plenum, New York, 1986).

[8]J. J. Rush, J. M. Rowe, and A. J. Maeland, J. Phys. F **10**, L283 (1980).

[9]H. Kaneko, T. Kajitani, M. Hirabayashi, M. Ueno, and K. Suzuki, J. Less-Common Met. **89**, 237 (1983).

[10]K. Suzuki, N. Hayashi, Y. Tomizuka, T. Sukunaga, K. Kai, and N. Watanabe, J. Non-Cryst. Solids **61/62**, 637 (1984); K. Suzuki, J. Less-Commun. Met. **89**, 183 (1983).

[11]B. S. Berry and W. C. Pritchet, Scr. Metall. **15**, 637 (1981).

[12]R. Kirchheim, F. Sommer, and G. Schluckebier, Acta Metall. **30**, 1059 (1982).

[13]R. Kircheim, Acta Metall. **30**, 1069 (1982).

[14]A. C. Switendick, Z. Phys. Chem. Neue Folge **117**, 89 (1979).

[15]B. H. Mahan, *University Chemistry,* 3rd ed. (Addison-Wesley, Reading, MA, 1975), p. 342.

[16]J. L. Finney and J. Wallace, in *Proceedings of the 4th International Conference on Rapidly Quenched Metals,* Ref. 1(a), p. 253.

[17]This idea, but without a variety of site types, has been employed in Ref. 12 and by R. Griessen, Phys. Rev. B **27**, 7575 (1983) and P. M. Richards, Phys. Rev. B **30**, 5183 (1984). In Ref. 2, two site types, the B_4 and AB_3 sites, appear to be included.

[18]P. S. Rudman and G. D. Sandrock, Ann. Rev. Mater. Sci. **12**, 271 (1982).

[19]P. Panissod and T. Mizoguchi, in *Proceedings of the 4th International Conference on Rapidly Quenched Metals,* Ref. 1(a), p. 1621.

[20]H. Fujimori, K. Nakanishi, K. Shirikawa, T. Masumoto, T. Kaneko, and N. S. Kazama, in *Proceedings of the 4th International Conference on Rapidly Quenched Metals,* Ref. 1(a), p. 1629.

[21]B. Rodmacq, A. K. Bhatnagar, and A. Chamberod, J. Phys. F **16**, L259 (1986).

[22]W. A. Oates, J. A. Lambert, and P. T. Gallagher, Trans. Metall. Soc. AIME **47**, 245 (1969).

[23]Other blocking schemes in amorphous alloys have been considered to some extent in Refs. 2 and 5 but with limited success. See also P. M. Richards, Phys. Rev. B **30**, 5183 (1984).

[24]D. Nelson, Sci. Am., August, 43 (1986).

[25]D. R. Nelson, Phys. Rev. B **28**, 5515 (1983).

[26]P. J. Steinhardt, D. R. Nelson, and M. Ronchetti, Phys. Rev. B **28**, 784 (1983).

[27]W. A. Curtin and J. H. Harris, Proceedings of the 6th International Conference on Rapidly Quenched Metals (unpublished).

[28]E. Hellstern and L. Schultz, Appl. Phys. Lett. **48**, 124 (1986).

[29]A. K. Sinha, in *Topologically Close-Packed Structures of Transition Metal Alloys,* edited by B. Chalmers, J. W. Christian and T. B. Massalki (Pergamon, Oxford, 1972).

[30]D. Ivey and D. Northwood, J. Less-Common. Met. **115**, 23 (1986).